

Infection of brain pericytes underlying neuropathology of COVID-19 patients

Matteo Bocci,^{1†} Clara Oudenaarden,^{1†} Xavier Sàenz-Sardà,² Joel Simrén,³ Arvid Edén,^{4,5}
Jonas Sjölund,¹ Christina Möller,¹ Magnus Gisslén,^{4,5} Henrik Zetterberg,^{3,6,7,8} Elisabet
Englund² and Kristian Pietras^{1*}

†These authors contributed equally to this work.

Abstract

A wide range of neurological manifestations have been associated with the development of COVID-19 following SARS-CoV-2 infection. However, the etiology of the neurological symptomatology is still largely unexplored.

Here, we used state-of-the-art multiplexed immunostaining of human brains ($n = 6$ COVID-19, median age = 69,5 years; and $n = 7$ control, median age = 68 years), and demonstrated that expression of the SARS-CoV-2 receptor ACE2 is restricted to a subset of neurovascular pericytes. Strikingly, neurological symptoms were exclusive to, and ubiquitous in, patients that exhibited moderate to high ACE2 expression in peri-vascular cells. Viral particles were identified in the vascular wall and paralleled by peri-vascular inflammation, as signified by T cell and macrophage infiltration. Furthermore, fibrinogen leakage indicated compromised integrity of the blood-brain barrier. Notably, cerebrospinal fluid from an additional 16 individuals ($n = 8$ COVID-19, median age = 67 years; and $n = 8$ control, median age = 69,5 years) exhibited significantly lower levels of the pericyte marker PDGFR β in SARS-CoV-2-infected cases, indicative of disrupted pericyte homeostasis.

We conclude that pericyte infection by SARS-CoV-2 underlies virus entry into the privileged central nervous system space, as well as neurological symptomatology due to peri-vascular inflammation and a locally compromised blood-brain barrier.

Author affiliations:

1 Department of Laboratory Medicine, Division of Translational Cancer Research, Lund University Cancer Centre, Medicon Village, Lund University, 223 81 Lund, Sweden.

2 Department of Clinical Sciences Lund, Division of Pathology, Lund University, 221 84 Lund, Sweden.

3 Department of Psychiatry and Neurochemistry, Institute of Neuroscience & Physiology, The Sahlgrenska Academy at the University of Gothenburg, 431 41 Gothenburg, Sweden.

4 Department of Infectious Diseases, Institute of Biomedicine, The Sahlgrenska Academy at the University of Gothenburg, 413 46 Gothenburg, Sweden.

5 Region Västra Götaland, Sahlgrenska University Hospital, Department of Infectious Diseases, 416 50 Gothenburg, Sweden.

6 Clinical Neurochemistry Laboratory, Sahlgrenska University Hospital, 431 80 Gothenburg, Sweden.

7 Department of Neurodegenerative Disease, UCL Institute of Neurology, WC1N 3BG London, UK.

8 UK Dementia Research Institute at UCL, WC1E 6BT London, UK.

Correspondence to:
Kristian Pietras, Ph.D.
Grosskopf Professor of Molecular Medicine
Lund University
Department of Laboratory Medicine
Division of Translational Cancer Research
Medicon Village, Building 404:A3
SE-223 81 Lund, Sweden
Phone +46 709 209 709
E-mail Kristian.Pietras@med.lu.se
Twitter @KPietraslab

Running title: Perivascular SARS-CoV-2 infection in the brain

Keywords: COVID-19; pericytes; blood-brain barrier; multiplexed IHC; infection

Abbreviations: BBB = blood-brain barrier; COVID-19 = coronavirus disease 2019; CSF = cerebrospinal fluid; HIER = heat-induced epitope retrieval; mIHC = multiplexed immunohistochemistry; SARS-CoV-2 = severe acute respiratory syndrome coronavirus 2.

Introduction

The clinical manifestations of coronavirus disease 2019 (COVID-19) infection primarily include respiratory symptoms, ranging from a mild cough to severe bilateral pneumonia^{1, 2}. However, SARS-CoV-2 bears an organotropism beyond the respiratory tract^{3, 4}, with increasing testimony indicating the brain as an extrapulmonary target of SARS-CoV-2⁵. The involvement of the CNS encompasses a broad spectrum of neurological manifestations (including headache, fatigue, anosmia, ageusia, confusion, loss of consciousness), often representing an ulterior clinical morbidity that significantly contributes to COVID-19-related deaths⁶⁻⁸.

The main entry receptor for SARS-CoV-2 is reported to be the angiotensin-converting enzyme (ACE)2, which is a component of the renin-angiotensin system^{9, 10}. To date there is still no conclusive evidence concerning the localization of ACE2 in the human CNS³, and the mechanism of SARS-CoV-2 infection in the brain remains a conundrum.

Here, using highly sensitive multiplexed immunohistochemistry (mIHC) of brain tissue from a series of confirmed COVID-19 patients and corresponding controls, we determined that ACE2 is exclusively expressed by brain pericytes in the subset of patients that also exhibited neurological symptoms. Moreover, spatial immunophenotyping revealed a localized perivascular inflammation in brain tissue from COVID-19 patients, paralleled by an impairment of the functionality of the vascular wall as indicated by loss of integrity of the blood-brain barrier (BBB). Finally, in the cerebrospinal fluid (CSF) of a cohort of COVID-19 patients with neurological involvement, levels of soluble PDGFR β , a pericyte-specific marker in the brain, were significantly reduced compared with non-COVID-19 individuals, suggestive of SARS-CoV-2-related functional impairment of pericytes. Taken together, our findings highlight a previously unappreciated role for brain pericytes in acting as pioneers for SARS-CoV-2 entry into the CNS.

Materials and methods

Patients

Excessive brain tissues sampled from six COVID-19 autopsies and 7 non-COVID-19 cases were used to create formalin-fixed paraffin-embedded (FFPE) blocks (Supplementary Table 1). The use of these samples was approved by the Central Ethical Review Authority in Sweden (2020-02369, 2020-06582, and 2020-01771). Clinical data with details of neurologic symptoms or other signs of brain affection were sought in the referral documents or else in the Regional Medical Records database Melior, which was used also for the diagnostic work-up.

CSF from eight patients with neurological manifestations admitted to the Sahlgrenska University Hospital in Gothenburg, Sweden was included (Supplementary Table 2). Infection with SARS-CoV-2 was confirmed *via* rtPCR analysis. Age- and sex-matched non-COVID-19 controls were selected, consisting of patients who were examined because of clinical suspicion of neurological disease, but where no neurochemical evidence was found, based on clinical reference intervals. The use of these samples has been approved by the Regional Ethical Committee in Gothenburg.

Bioinformatics data access and analysis

Expression of *Ace2* was investigated in publicly available single cell RNA sequencing (scRNA-seq) SMART-Seq2 RNA-seq libraries on FACS-sorted non-myeloid brain cells of seven mice (*Tabula Muris*)¹¹, and in a database of murine vasculature^{12, 13}.

Mouse whole brain and hippocampus SMART-seq data (gene expression aggregated per cluster, calculated as trimmed means) from the Allen Brain Atlas consortium was downloaded on 14th October 2020^{14, 15}. For expression of *Pvalb* and *Sst* neurons, the average was calculated of 13 and 40 cell clusters, respectively.

Human ACE2 protein expression images were retrieved from the Human Protein Atlas initiative (Version 20.0)¹⁶.

Immunohistochemistry (IHC)

Five µm-thick FFPE tissue sections were dewaxed and rehydrated through xylene and water-based ethanol solutions. Heat-induced epitope retrieval was performed with a pressure cooker (2100 Antigen Retriever, BioVendor, Germany) in citrate or Tris-EDTA buffer (Agilent Dako, USA). Following endogenous peroxidase quenching (BLOXALL, Vector Laboratories, USA), tissues were incubated with CAS-block (Thermo Fisher Scientific, USA), 1 hour at room temperature (RT), and Ultra V block (Thermo Fisher Scientific, USA) for 5 minutes. Primary antibodies (Supplementary Table 3) diluted in CAS-block were applied for 30 minutes, followed by UltraVision ONE HRP polymer (Thermo Fisher Scientific, USA), 30 minutes, at RT. The ImmPACT DAB substrate (Vector Laboratories, USA) was applied. Tissues were counterstained with hematoxylin, dehydrated and mounted with Cytoseal 60 (Thermo Fisher Scientific, USA). Imaging was performed with an automated BX63 microscope connected to a DP-80 camera (Olympus, Japan).

Multiplexed IHC (mIHC)

FFPE sections used for IHC were subjected to multiplexed labelling following optimized protocols established in the lab. All reagents are from Akoya Biosciences (USA), including the Vectra Polaris scanner for imaging and the PhenoChart/InForm software. Following slide preparation, sections underwent staining cycles (Supplementary Table 4) —including blocking, primary antibody incubation, HRP tagging and labeling with OPAL-conjugated tyramide substrate— and a stripping procedure to remove unbound primary antibody/HRP. A counterstain with DAPI preceded the mounting with ProLong Diamond antifade (Thermo Fisher Scientific, USA).

The composite images were generated by removing inherent autofluorescence signal from an unstained section, as well as by comparing fluorescence intensities to those of a spectral library.

Soluble PDGFR β ELISA

CSF sPDGFR β concentration was measured by sandwich ELISA (Thermo Fisher Scientific, USA), as previously described¹⁷. Statistical Mann-Whitney U-test was performed using Prism (GraphPad Software, USA). The significance level was set at $P < 0.05$, two-sided.

Data availability

The authors confirm that the data supporting the findings of this study are available within the article and its supplementary material.

Results

The ACE2 receptor is expressed by pericytes in murine and human brain

Expression of ACE2 in the brain has variably been reported in neurons, glial cells, and vascular cells¹⁸⁻²². Because of this ambiguity of localization, we started by exploring ACE2 expression in publicly available mRNA and protein datasets from murine and human brain. Mining of the Allen Mouse Brain Atlas of single cell transcriptomes demonstrated unique enrichment for *Ace2* transcript in pericytes (Fig. 1A). A similar compartmentalization was observed in the *Tabula Muris*¹¹ as well as in an scRNA-seq compendium of the murine brain vasculature^{12, 13} (Supplementary Fig. 1A and B). In agreement with the transcriptional data, localization of the ACE2 protein by the Human Protein Atlas¹⁶ was restricted to the peri-vascular compartment in a subset of blood vessels in human cerebral cortex (Supplementary Fig. 1C).

The ACE2 protein is expressed by peri-vascular cells of neural tissue from COVID-19 patients with neurological symptoms

Next, we sought to investigate the expression of ACE2 in brain tissue of COVID-19 patients. To this end, we obtained FFPE samples of multiple brain regions from six patients whose death was confirmed to be a consequence of SARS-CoV-2 infection (Supplementary Table 1). In the frontal cortex, moderate to high ACE2 immunoreactivity revealed a vascular pattern in a subset of blood vessels in five of the 13 cases (Fig. 1B). Reassuringly, other brain regions showed equivalent distribution of ACE2, indicating that ACE2 was widely expressed in peri-vascular cells throughout the CNS (Fig. 1C). Notably, ACE2 reactivity, which was confirmed with two different antibodies in positive control tissues from kidney (Supplementary Fig. 1D), appeared to be a patient-specific feature, since some cases did not show signal at all, or with very low frequency (Fig. 1D and Supplementary Fig. 1E). To conclusively validate which cell type harbored ACE2 expression, we performed mIHC on human brain tissue to simultaneously

visualize ACE2, CD31⁺ endothelial cells, PDGFR β ⁺ pericytes. ACE2 expression coincided with that of PDGFR β , but not with CD31 staining (Fig. 1E and Supplementary Fig. 1F). Pericytes investing the vasculature exhibited a nuanced pattern of PDGFR β and ACE2 immunoreactivity, with some cells bearing positivity solely for PDGFR β , while others expressed both markers. Remarkably, the three COVID-19 patients that exhibited moderate to high peri-vascular ACE2 expression in the brain all presented with neurological symptoms, while all ACE2-negative patients remained free from such manifestations (Fig. 1D). Collectively, our data demonstrate that in the brain, ACE2 is exclusively expressed by pericytes in a manner that signifies development of neurological symptoms from COVID-19.

SARS-CoV-2 is detectable in human brain of COVID-19 patients

An increasing body of evidence converges on the inherent difficulty of detecting SARS-CoV-2 in the brain^{23, 24}. To build on previous reports on the localization of SARS-CoV-2 in human brain tissue, we additionally analyzed brain samples from non-infected individuals to enable conclusions about the presence of the spike protein or the nucleocapsid protein of SARS-CoV/SARS-CoV-2 in the CNS with a higher certainty. For both viral components, positive areas in brain sections of COVID-19 patients exhibited comparable patterns with those shown in previous studies.²⁵ Notably, however, we demonstrated an analogous intensity and distribution of the viral proteins when we probed brain tissues from non-infected individuals (Fig. 2A). In order to unequivocally define our ability to visualize viral particles in human tissues, we gained access to placental tissue from a confirmed case of SARS-CoV-2 vertical transmission to serve as a positive control²⁶. We also made use of the J2 antibody specifically designed to detect viral double-stranded (ds)RNA. In the placenta, a 7-plex mIHC panel confirmed the epithelial cytokeratin⁺ syncytiotrophoblasts as the main target for viral infection by virtue of expression of ACE2 and the presence of dsRNA in a well-defined dotted pattern (Fig. 2B and Supplementary Fig. 2A); a pattern of distribution which was essentially preserved

with antibodies against the coronaviridae family or SARS-CoV-2-specific antigens (Supplementary Fig. 2B). Finally, applying the now validated protocol for detection of viral dsRNA to brain sections, we identified an analogous dotted pattern in discrete peri-vascular, non-endothelial, cells in the brain of COVID-19 patients (Fig. 2C and Supplementary Fig. 2C). Reassuringly, the peri-vascular staining pattern was absent from brain samples of non-infected individuals. Together with our observations of ACE2 expression in pericytes, our conclusive localization of viral dsRNA suggests that brain pericytes are indeed uniquely susceptible to viral infection and may serve as CNS entry points for SARS-CoV-2.

Peri-vascular infection by SARS-CoV-2 in the brain is paralleled by peri-vascular inflammation

We hypothesized that infection of pericytes would result in neuro-inflammation and therefore implemented a spatial immunophenotyping approach for the concomitant detection of the endothelium (CD34⁺) and five immune cell populations, including T helper and cytotoxic T lymphocytes, regulatory T cells, B cells, and macrophages. Surrounding the brain vasculature in COVID-19 patients, we detected CD4⁺ and CD8⁺ T cells, as well as CD68⁺ macrophages, indicative of peri-vascular inflammation, rather than widespread neuroinflammation in the brain parenchyme (Fig. 2D and Supplementary Fig. 2D). The immune infiltration did not affect all blood vessels, indicating that the inflammation was not the result of systemic mediators, but rather of local instigation.

Pericyte infection leads to vascular fibrinogen leakage in the CNS

Next, we investigated whether impaired pericyte function consequential to SARS-CoV-2 infection and the peri-vascular inflammation impinged on the integrity of the vascular wall. We first performed a 7-plex mIHC staining focusing on the permeability of the neurovascular unit. Remarkably, in COVID-19 patients, extra-vascular fibrinogen was readily detected as a

characteristic gradient in subsets of vessels, occasionally also characterized by ACE2 expression and the presence of viral dsRNA (Fig. 3A and Supplementary Fig. 3 A and B). Conversely, fibrinogen was fully retained within the blood vessels of non-infected control cases. Moreover, astrocyte priming indicative of local activation of the brain parenchyme was not apparent during COVID-19 infection (Fig. 3B and Supplementary Fig. 3C). Together with our identification of SARS-CoV-2 and immune cell infiltrates in the peri-vascular region, the leakage of fibrinogen from the blood vessels strongly suggests that viral infection of pericytes breaches the tightly organized BBB.

Shedding of PDGFR β into the CSF is reduced in COVID-19 patients

Our findings led us to speculate that the homeostatic state of brain pericytes would be disrupted in COVID-19 patients. Therefore, we collected CSF from an additional eight patients with acute COVID-19 that presented with neurological manifestations, as well as non-infected matched controls (Supplementary Table 2). Intriguingly, the level of the pericyte marker sPDGFR β in the CSF of COVID-19 patients was on average significantly lower than in non-COVID-19 control individuals as measured by ELISA, indicative of a perturbed pericyte homeostasis (Fig. 3C).

Discussion

The primary cellular receptor for SARS-CoV-2 entry is ACE2⁹, but the expression pattern of ACE2 in the CNS has not been conclusively resolved. Notably, the few published studies detailing the expression of ACE2 and/or SARS-CoV-2 protein in the CNS lack reliable and appropriate controls, precluding firm conclusions. Here, by means of highly sensitive mIHC and the use of both positive and negative control tissues, we were able to confirm that ACE2 exhibited an exclusive peri-vascular expression pattern in the CNS. Similarly, viral particles and their dsRNA were observed in CNS pericytes in COVID-19 patients, independently of the peri-vascular ACE2 expression status. Whether other co-receptors for SARS-CoV-2, including TMPRSS2, CD147, and neuropilin-1, contribute to CNS-tropism remains to be investigated.

Based on our observations, we hypothesize that infection and subsequent damage of brain vascular pericytes by SARS-CoV-2 and peri-vascular inflammation may lead to impairment of the BBB, instigating neurological complications and possibly virus entry into the CNS. In line with our report, two recent studies observed vascular leakage and peri-vascular immune infiltration in the brain of COVID-19 patients, but without the crucial link to ACE2 expression by, and infection of, pericytes^{27,28}. However, it is still an outstanding question whether SARS-CoV-2 is overtly neurotropic or if the neurological symptoms associated with COVID-19 are secondary to events related to the systemic host response²⁹. Although solely based on the comparable abundance of GFAP in the tissues, our observations do not provide support for the hypothesis of a cytokine storm. Nevertheless, immune activation markers β 2-microglobulin and neopterin were previously found to be elevated in the CSF of COVID-19 patients³⁰. Hence, further investigations are warranted to fully clarify whether a systemic inflammatory response is associated with neurological manifestations of COVID-19.

Intriguingly, COVID-19 patients with neurological symptoms presented with a reduced concentration of pericyte-derived sPDGFR β in the CSF. While our mIHC of brain tissue demonstrated a surprisingly variable occurrence of PDGFR β^+ peri-vascular cells, in line with the results from the CSF analysis, the analysis did not support an overall diminished pericyte coverage of the vasculature of COVID-19 patients. A second, and perhaps more likely, explanation for the reduced expression/shedding of PDGFR β in COVID-19 patients, is that SARS-CoV-2 infection of pericytes diverted the protein synthesis machinery to produce viral proteins, leading to loss of endogenous marker expression³¹ and consequential functional impairment.

An improved understanding of SARS-CoV-2 neurotropism is urgently needed to guide the clinical management of acute neurological symptoms, as well as to define strategies to prevent post-infectious neurological complications. We propose that a possible entry site of SARS-CoV-2 into the CNS goes through ACE2-expressing pericytes. Interestingly, although overt endothelial cell infection by SARS-CoV-2 does not appear to occur²², a recent investigation determined that radiolabeled S1 spike viral protein could be retained on the abluminal side of endothelial cells where it associated with the capillary glycocalyx in mice or further sequestered by the endothelium³². It is thus tempting to speculate that this represents one plausible way to expose pericytes to the viral infection. Furthermore, the absence of brain pericytes in mice results in a disrupted BBB associated with wide-spread loss of integrity³³. Conversely, sealing of the BBB following thrombolysis after ischemic stroke has been achieved in clinical trials by treatment with the tyrosine kinase inhibitor imatinib^{34,35}. Whether similar interventions aiming to support the integrity of the BBB would alleviate neurological symptoms in COVID-19 patients warrants further studies.

Acknowledgements

We gratefully acknowledge Professor David Gisselsson Nord (Lund University) for provision of placenta tissue specimens, and associate professor Emma Hammarlund (Lund University) for critically reading the manuscript.

Funding

KP is the Göran and Birgitta Grosskopf Professor of Molecular Medicine and is supported by grants from the Swedish Research Council (#2018-03086), Swedish State Support for Clinical Research through Region Skåne ALF, the Göran Gustafsson foundation, the Mats Paulsson foundations, and the Cancera foundation. HZ is a Wallenberg Scholar supported by grants from the Swedish Research Council (#2018-02532), the European Research Council (#681712), Swedish State Support for Clinical Research (#ALFGBG-720931), the Alzheimer Drug Discovery Foundation (ADDF), USA (#201809-2016862), the AD Strategic Fund and the Alzheimer's Association (#ADSF-21-831376-C, #ADSF-21-831381-C and #ADSF-21-831377-C), the Olav Thon Foundation, the Erling-Persson Family Foundation, Stiftelsen för Gamla Tjänarinnor, Hjärnfonden, Sweden (#FO2019-0228), the European Union's Horizon 2020 research and innovation programme under the Marie Skłodowska-Curie grant agreement No 860197 (MIRIADE), and the UK Dementia Research Institute at UCL. MG is supported by The Swedish State Support for Clinical Research (ALFGBG-717531) and by SciLifeLab Sweden (KAW 2020.0182). JS has received support from Stiftelsen för Gamla Tjänarinnor and Stohnes stiftelse. EE and XSS were supported by Region Skåne, Sweden.

Competing interests

KP is a scientific advisor for Baxter and Pfizer, recipient of research grants from Acceleron Pharma, and a minority stock owner of Paracrine Therapeutics. HZ has served at scientific

advisory boards for Denali, Roche Diagnostics, Wave, Samumed, Siemens Healthineers, Pinteon Therapeutics, Nervgen and CogRx, has given lectures in symposia sponsored by Fujirebio, Alzecure and Biogen, and is a co-founder of Brain Biomarker Solutions in Gothenburg AB (BBS), which is a part of the GU Ventures Incubator Program (outside submitted work).

Supplementary material

Supplementary material is available at *Brain* online.

References

1. Chen N, Zhou M, Dong X, et al. Epidemiological and clinical characteristics of 99 cases of 2019 novel coronavirus pneumonia in Wuhan, China: a descriptive study. *Lancet*. Feb 15 2020;395(10223):507-513. doi:10.1016/S0140-6736(20)30211-7
2. Wang D, Hu B, Hu C, et al. Clinical Characteristics of 138 Hospitalized Patients With 2019 Novel Coronavirus-Infected Pneumonia in Wuhan, China. *JAMA*. Mar 17 2020;323(11):1061-1069. doi:10.1001/jama.2020.1585
3. Puelles VG, Lutgehetmann M, Lindenmeyer MT, et al. Multiorgan and Renal Tropism of SARS-CoV-2. *N Engl J Med*. Aug 6 2020;383(6):590-592. doi:10.1056/NEJMc2011400
4. Gupta A, Madhavan MV, Sehgal K, et al. Extrapulmonary manifestations of COVID-19. *Nat Med*. Jul 2020;26(7):1017-1032. doi:10.1038/s41591-020-0968-3
5. Paterson RW, Brown RL, Benjamin L, et al. The emerging spectrum of COVID-19 neurology: clinical, radiological and laboratory findings. *Brain*. Oct 1 2020;143(10):3104-3120. doi:10.1093/brain/awaa240
6. Helms J, Kremer S, Merdji H, et al. Neurologic Features in Severe SARS-CoV-2 Infection. *N Engl J Med*. Jun 4 2020;382(23):2268-2270. doi:10.1056/NEJMc2008597
7. Mao L, Jin H, Wang M, et al. Neurologic Manifestations of Hospitalized Patients With Coronavirus Disease 2019 in Wuhan, China. *JAMA Neurol*. Jun 1 2020;77(6):683-690. doi:10.1001/jamaneurol.2020.1127
8. Oxley TJ, Mocco J, Majidi S, et al. Large-Vessel Stroke as a Presenting Feature of Covid-19 in the Young. *N Engl J Med*. May 14 2020;382(20):e60. doi:10.1056/NEJMc2009787
9. Hoffmann M, Kleine-Weber H, Schroeder S, et al. SARS-CoV-2 Cell Entry Depends on ACE2 and TMPRSS2 and Is Blocked by a Clinically Proven Protease Inhibitor. *Cell*. Apr 16 2020;181(2):271-280 e8. doi:10.1016/j.cell.2020.02.052
10. Li MY, Li L, Zhang Y, Wang XS. Expression of the SARS-CoV-2 cell receptor gene ACE2 in a wide variety of human tissues. *Infect Dis Poverty*. Apr 28 2020;9(1):45. doi:10.1186/s40249-020-00662-x

11. Tabula Muris C, Overall c, Logistical c, et al. Single-cell transcriptomics of 20 mouse organs creates a Tabula Muris. *Nature*. Oct 2018;562(7727):367-372. doi:10.1038/s41586-018-0590-4
12. Vanlandewijck M, He L, Mae MA, et al. A molecular atlas of cell types and zonation in the brain vasculature. *Nature*. Feb 22 2018;554(7693):475-480. doi:10.1038/nature25739
13. He L, Vanlandewijck M, Mae MA, et al. Single-cell RNA sequencing of mouse brain and lung vascular and vessel-associated cell types. *Sci Data*. Aug 21 2018;5:180160. doi:10.1038/sdata.2018.160
14. Lein ES, Hawrylycz MJ, Ao N, et al. Genome-wide atlas of gene expression in the adult mouse brain. *Nature*. Jan 11 2007;445(7124):168-76. doi:10.1038/nature05453
15. Allen Mouse Brain Atlas [Internet]. Seattle (WA): Allen Institute for Brain Science. ©2011. Available from: . <https://portal.brain-map.org/atlasses-and-data/rnaseq/human-multiple-cortical-areas-smart-seq>
16. Uhlen M, Fagerberg L, Hallstrom BM, et al. Proteomics. Tissue-based map of the human proteome. *Science*. Jan 23 2015;347(6220):1260419. doi:10.1126/science.1260419
17. Miners JS, Kehoe PG, Love S, Zetterberg H, Blennow K. CSF evidence of pericyte damage in Alzheimer's disease is associated with markers of blood-brain barrier dysfunction and disease pathology. *Alzheimers Res Ther*. Sep 14 2019;11(1):81. doi:10.1186/s13195-019-0534-8
18. Doobay MF, Talman LS, Obr TD, Tian X, Davisson RL, Lazartigues E. Differential expression of neuronal ACE2 in transgenic mice with overexpression of the brain renin-angiotensin system. *Am J Physiol Regul Integr Comp Physiol*. Jan 2007;292(1):R373-81. doi:10.1152/ajpregu.00292.2006
19. Xu J, Lazartigues E. Expression of ACE2 in Human Neurons Supports the Neuro-Invasive Potential of COVID-19 Virus. *Cell Mol Neurobiol*. Jul 4 2020;doi:10.1007/s10571-020-00915-1
20. Gallagher PE, Chappell MC, Ferrario CM, Tallant EA. Distinct roles for ANG II and ANG-(1-7) in the regulation of angiotensin-converting enzyme 2 in rat astrocytes. *Am J Physiol Cell Physiol*. Feb 2006;290(2):C420-6. doi:10.1152/ajpcell.00409.2004
21. Hamming I, Timens W, Bulthuis ML, Lely AT, Navis G, van Goor H. Tissue distribution of ACE2 protein, the functional receptor for SARS coronavirus. A first step in understanding SARS pathogenesis. *J Pathol*. Jun 2004;203(2):631-7. doi:10.1002/path.1570
22. McCracken IR, Saginc G, He L, et al. Lack of Evidence of ACE2 Expression and Replicative Infection by SARSCoV-2 in Human Endothelial Cells. *Circulation*. Jan 6 2021;doi:10.1161/CIRCULATIONAHA.120.052824
23. Matschke J, Lutgehetmann M, Hagel C, et al. Neuropathology of patients with COVID-19 in Germany: a post-mortem case series. *Lancet Neurol*. Nov 2020;19(11):919-929. doi:10.1016/S1474-4422(20)30308-2
24. Solomon IH, Normandin E, Bhattacharyya S, et al. Neuropathological Features of Covid-19. *N Engl J Med*. Sep 3 2020;383(10):989-992. doi:10.1056/NEJMc2019373
25. Bradley BT, Maioli H, Johnston R, et al. Histopathology and ultrastructural findings of fatal COVID-19 infections in Washington State: a case series. *Lancet*. Aug 1 2020;396(10247):320-332. doi:10.1016/S0140-6736(20)31305-2
26. Zaigham M, Holmberg A, Karlberg ML, et al. Intrauterine vertical SARS-CoV-2 infection: a case confirming transplacental transmission followed by divergence of the viral genome. *BJOG*. Feb 27 2021;doi:10.1111/1471-0528.16682
27. Lee M-H, Perl DP, Nair G, et al. Microvascular Injury in the Brains of Patients with Covid-19. *New England Journal of Medicine*. 2020;doi:10.1056/NEJMc2033369

28. Thakur KT, Miller EH, Glendinning MD, et al. COVID-19 neuropathology at Columbia University Irving Medical Center/New York Presbyterian Hospital. *Brain*. Apr 15 2021;doi:10.1093/brain/awab148
29. Pilotto A, Masciocchi S, Volonghi I, et al. SARS-CoV-2 encephalitis is a cytokine release syndrome: evidences from cerebrospinal fluid analyses. *Clin Infect Dis*. Jan 4 2021;doi:10.1093/cid/ciaa1933
30. Eden A, Kanberg N, Gostner J, et al. CSF biomarkers in patients with COVID-19 and neurological symptoms: A case series. *Neurology*. Oct 1 2020;doi:10.1212/WNL.0000000000010977
31. Banerjee AK, Blanco MR, Bruce EA, et al. SARS-CoV-2 Disrupts Splicing, Translation, and Protein Trafficking to Suppress Host Defenses. *Cell*. Nov 25 2020;183(5):1325-1339 e21. doi:10.1016/j.cell.2020.10.004
32. Rhea EM, Logsdon AF, Hansen KM, et al. The S1 protein of SARS-CoV-2 crosses the blood-brain barrier in mice. *Nat Neurosci*. Dec 16 2020;doi:10.1038/s41593-020-00771-8
33. Armulik A, Genove G, Mae M, et al. Pericytes regulate the blood-brain barrier. *Nature*. Nov 25 2010;468(7323):557-61. doi:10.1038/nature09522
34. Wahlgren N, Thoren M, Hojeberg B, et al. Randomized assessment of imatinib in patients with acute ischaemic stroke treated with intravenous thrombolysis. *J Intern Med*. Mar 2017;281(3):273-283. doi:10.1111/joim.12576
35. Su EJ, Fredriksson L, Geyer M, et al. Activation of PDGF-CC by tissue plasminogen activator impairs blood-brain barrier integrity during ischemic stroke. *Nat Med*. Jul 2008;14(7):731-7. doi:10.1038/nm1787

Figure legends

Figure 1 The ACE2 receptor is expressed by pericytes in murine and human brain. (A) Expression of *Ace2* in then annotated cell types in the mouse brain based on the Allen Mouse Brain Atlas. (B) Representative IHC staining of peri-vascular ACE2 in the frontal cortex of two COVID-19 patients and one control individual. Cell nuclei are counterstained with hematoxylin (blue). (C) Representative IHC staining of peri-vascular ACE2 in different brain regions of two COVID-19 patients. Cell nuclei are counterstained with hematoxylin (blue). (D) Clinical course of the COVID-19 patients included in the study. For each patient, appearance of symptoms, hospitalization, infection status and progression to death are included, together with the post-mortem evaluation of ACE2 immunoreactivity and thrombosis in the CNS. (E) Four-plex mIHC staining of the frontal cortex of a COVID-19 patient. The composite image depicts CD31 (endothelial cells, white), PDGFR β (pericytes, cyan), and ACE2 (orange). Cell nuclei are counterstained with DAPI (blue). In the inlets, the white arrows indicate ACE2-positive signal in the abluminal side of CD31. The intensity of each individual OPAL fluorophore, and the combined PDGFR β /ACE2 and CD31/ACE2 overlays are presented.

Figure 2 Peri-vascular infection by SARS-CoV-2 is paralleled by peri-vascular inflammation in the brain of COVID-19 patients. (A) Immunohistochemical detection of viral components in COVID-19-infected patients and non-COVID-19 controls. Cell nuclei are counterstained with hematoxylin (blue). The black arrows indicate the chromogenic deposition of the 3,3'-diaminobenzidine (DAB) substrate. (B) Representative field of a 7-plex mIHC staining panel of placental tissue infected with SARS-CoV-2. The magenta arrows indicate accumulation of viral dsRNA in correspondence of the ACE2-positive areas by the specialized epithelial layer of syncytiotrophoblast in the placenta. The intensity of each OPAL fluorophore is further presented in individual photomicrographs. (C) Immunohistochemical detection of dsRNA in the cerebral cortex of a COVID-19 patient and in a non-COVID-19 control. Cell

nuclei are counterstained with hematoxylin (blue). Black arrows indicate deposition of the DAB substrate. (D) Composite mIHC image of the peri-vascular immune cell infiltration in the frontal cortex of a COVID-19 patient and in a control individual. The antibody panel was designed for the concomitant detection of CD34 (endothelium) and five immune cell markers: CD4 (T helper cells), CD8 (cytotoxic T lymphocytes), CD20 (B cells), CD68 (macrophages), and FOXP3 (regulatory T cells).

Figure 3 Pericyte infection leads to vascular leakage in the CNS. (A) Composite mIHC of the frontal cortex of a COVID-19 patient and a control individual. The fields highlight the fibrinogen halo surrounding leaky blood vessels following SARS-CoV-2 infection. The images depict the neurovascular unit (CD34, PDGFR β , and ACE2), fibrinogen, viral dsRNA, and neurons. The intensity of each OPAL fluorophore is further presented in individual photomicrographs. The cyan arrows indicate fibrinogen leakage, yellow arrows highlight points of converging PDGFR β /dsRNA staining. (B) Composite mIHC of the frontal cortex of a COVID-19 patient and a control individual. The fields focus on astrocytes priming as a readout of local neuroinflammation. The images depict the neurovascular unit (CD34, PDGFR β , and ACE2), fibrinogen, SARS-CoV-2 spike protein, and astrocytes. (C) boxplot of the concentration of soluble PDGFR β (pg/ml) in the CSF of COVID-19 patients and non-COVID-19 controls (circles: individual measurements, cross: cohort average).

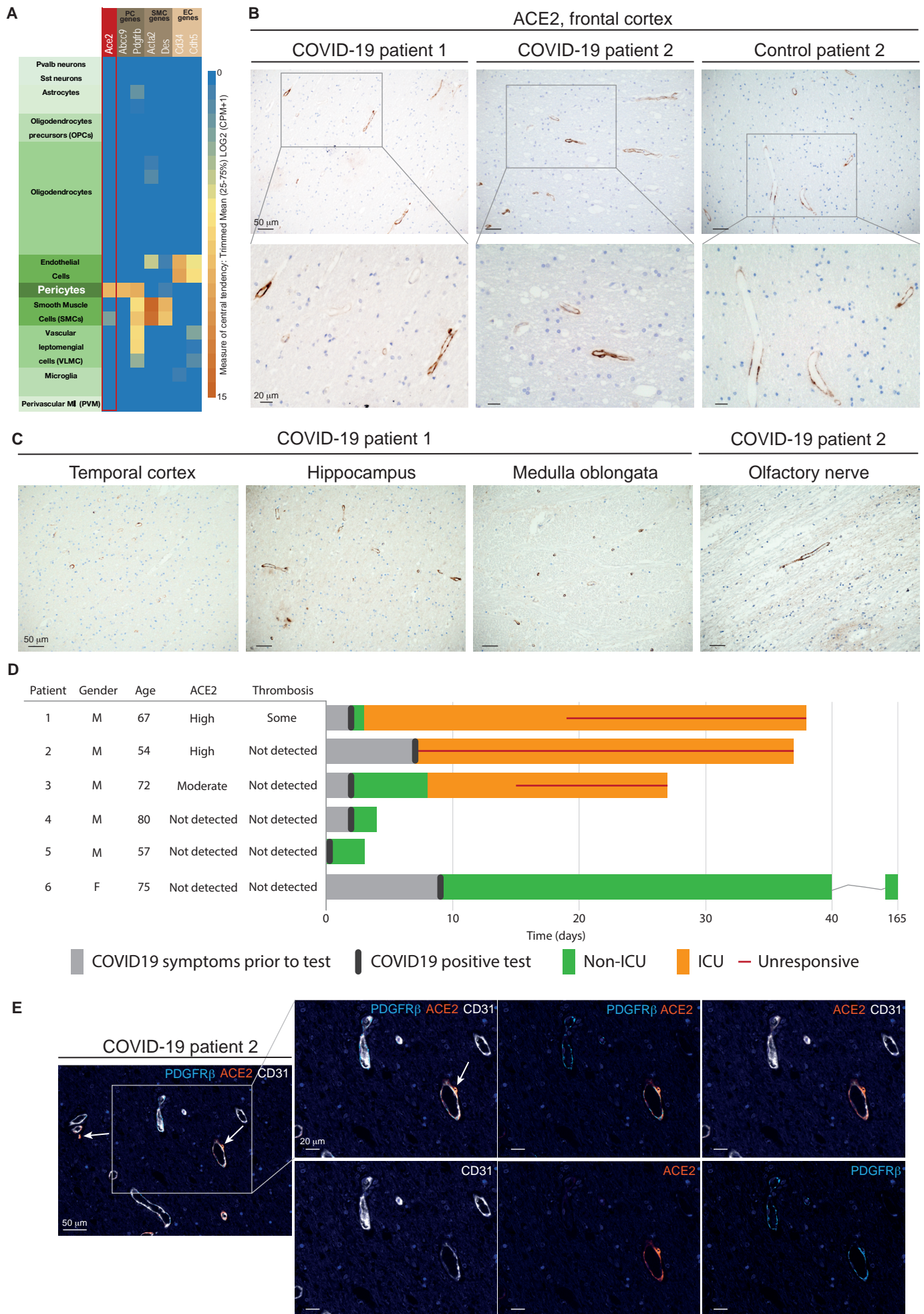
Supplementary Figure 1 (A) Feature plot of *Ace2* expression in seven distinct color-coded cell ontology classes (tissue reference: brain non-myeloid) from the *Tabula muris* compendium. (B) Enrichment for *Ace2* in mouse brain pericytes compared with other brain cell types based on the Betsholtz Atlas. (C) representative IHC staining of ACE2 in the cerebral cortex of three patients (and three antibodies) from the Human Protein Atlas initiative. Cell nuclei are counterstained with hematoxylin (blue). The black arrows indicate ACE2⁺ areas. (D) Representative IHC staining of ACE2 with two distinct antibodies in two different biopsies

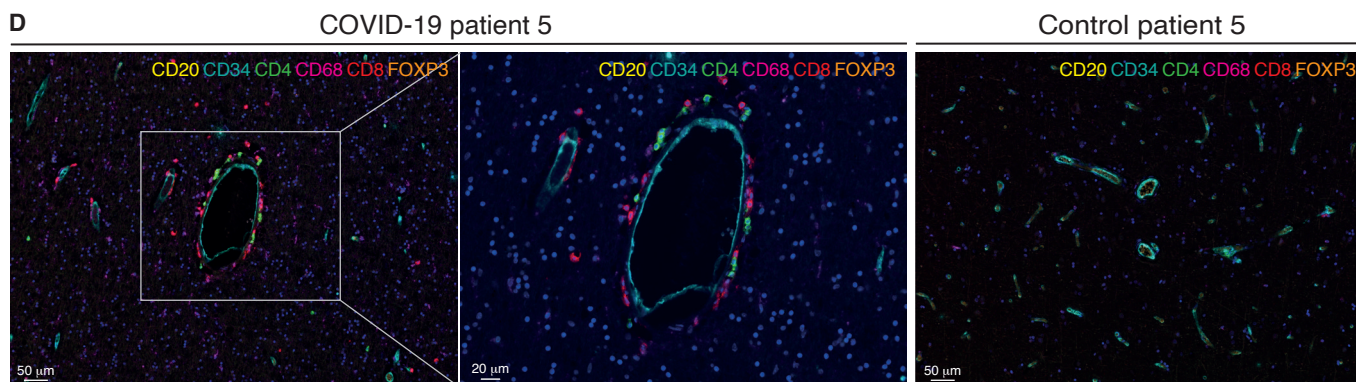
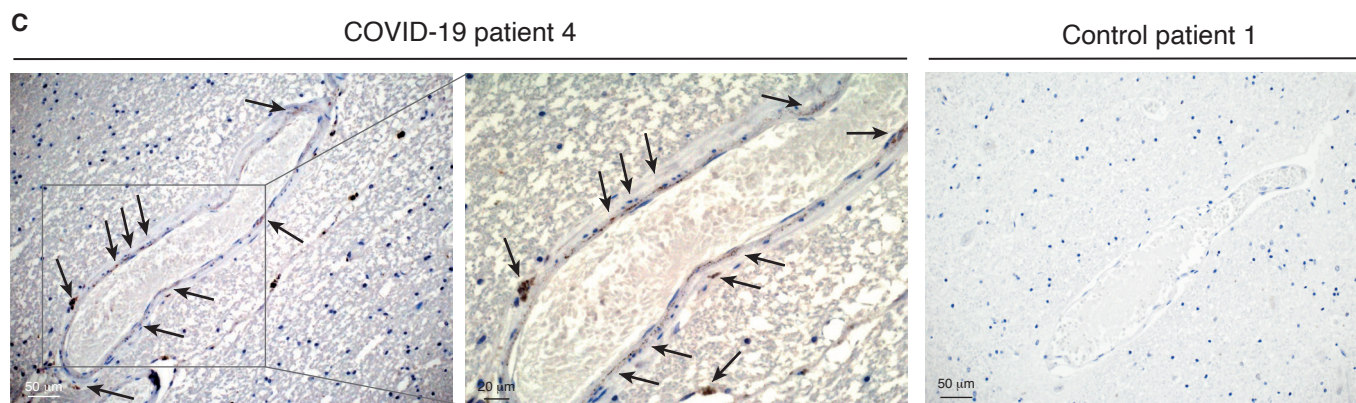
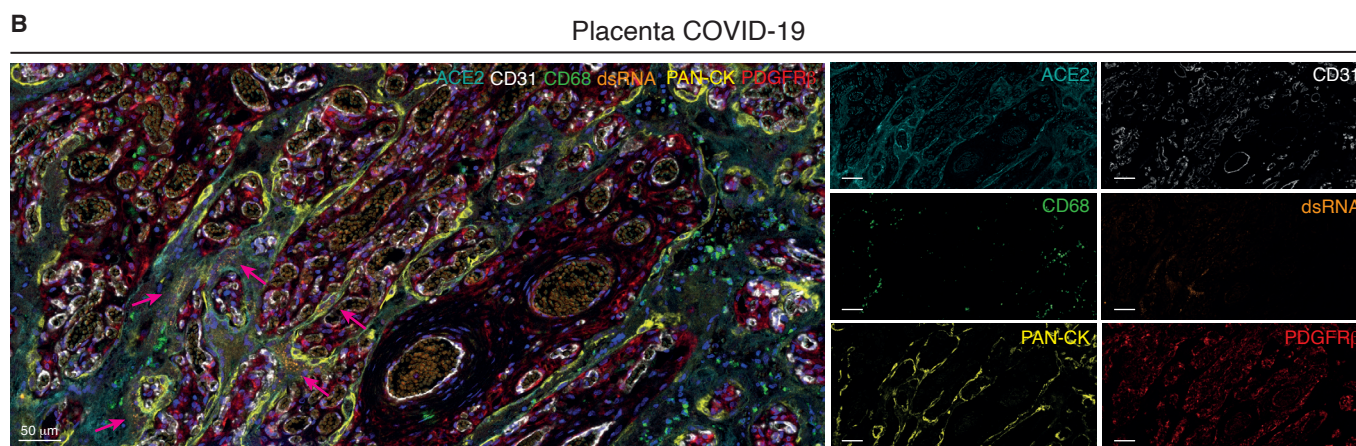
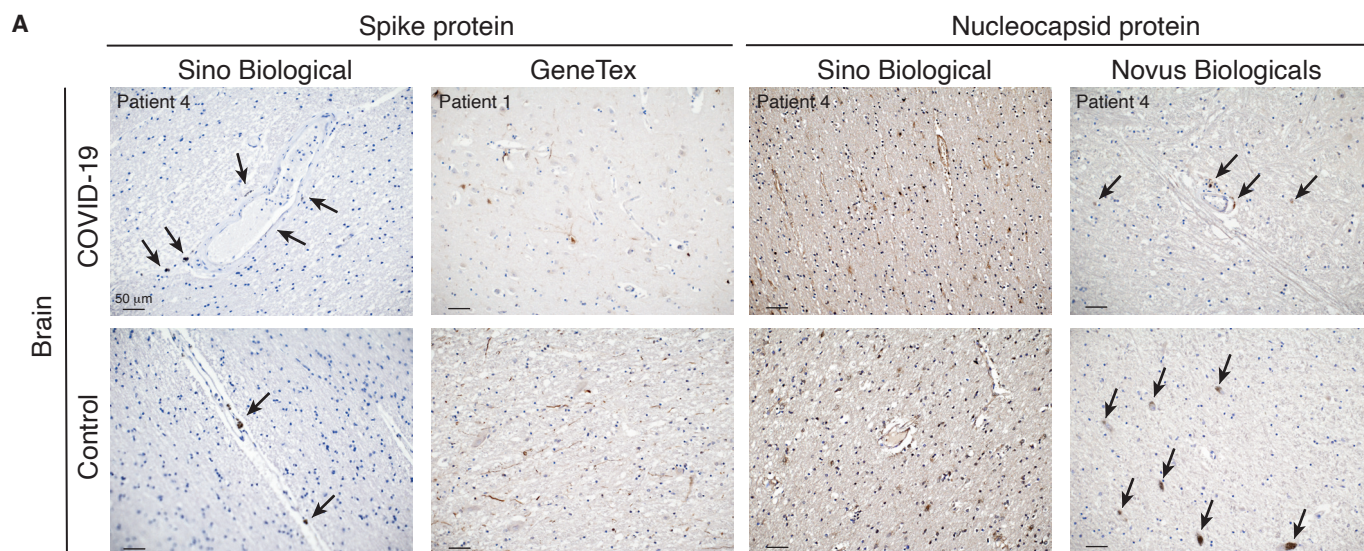
of human renal cell carcinoma. Cell nuclei are counterstained with hematoxylin (blue). **(E)** Representative IHC staining of peri-vascular ACE2 in the frontal cortex of one COVID-19 patients and two control individuals. Cell nuclei are counterstained with hematoxylin (blue). The black arrows indicate the chromogenic deposition of the DAB substrate. **(F)** Additional field of the 4-plex mIHC staining of the frontal cortex of the COVID-19 patient in Figure 1E. The final composite image depicts CD31 (endothelial cells, white), PDGFR β (pericytes, cyan), and ACE2 (orange). Cell nuclei are counterstained with DAPI (blue). In the inlets, the white arrows indicate ACE-positive signal in the abluminal side of CD31. The intensity of each individual OPAL fluorophore, and the combined PDGFR β /ACE2 and CD31/ACE2 overlays are presented.

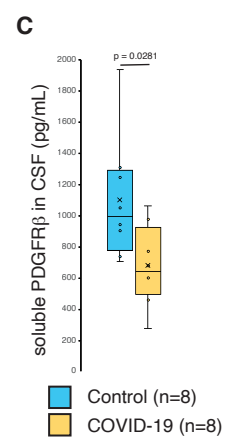
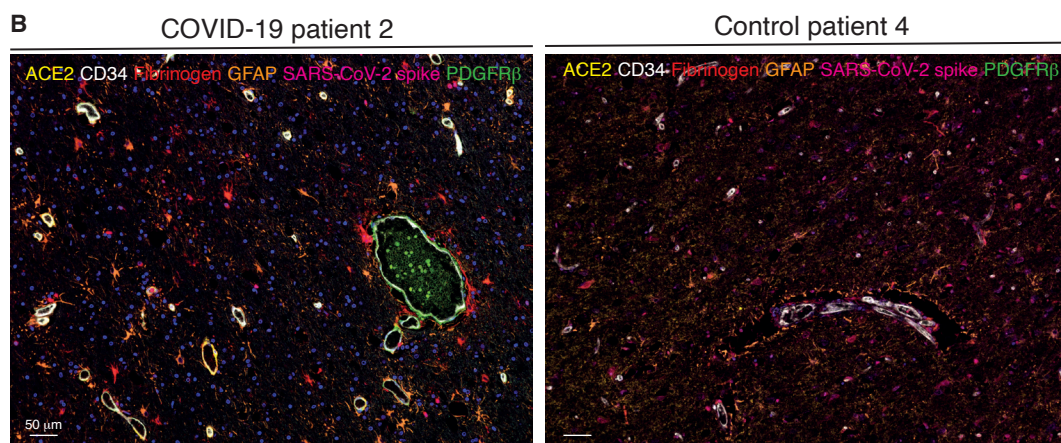
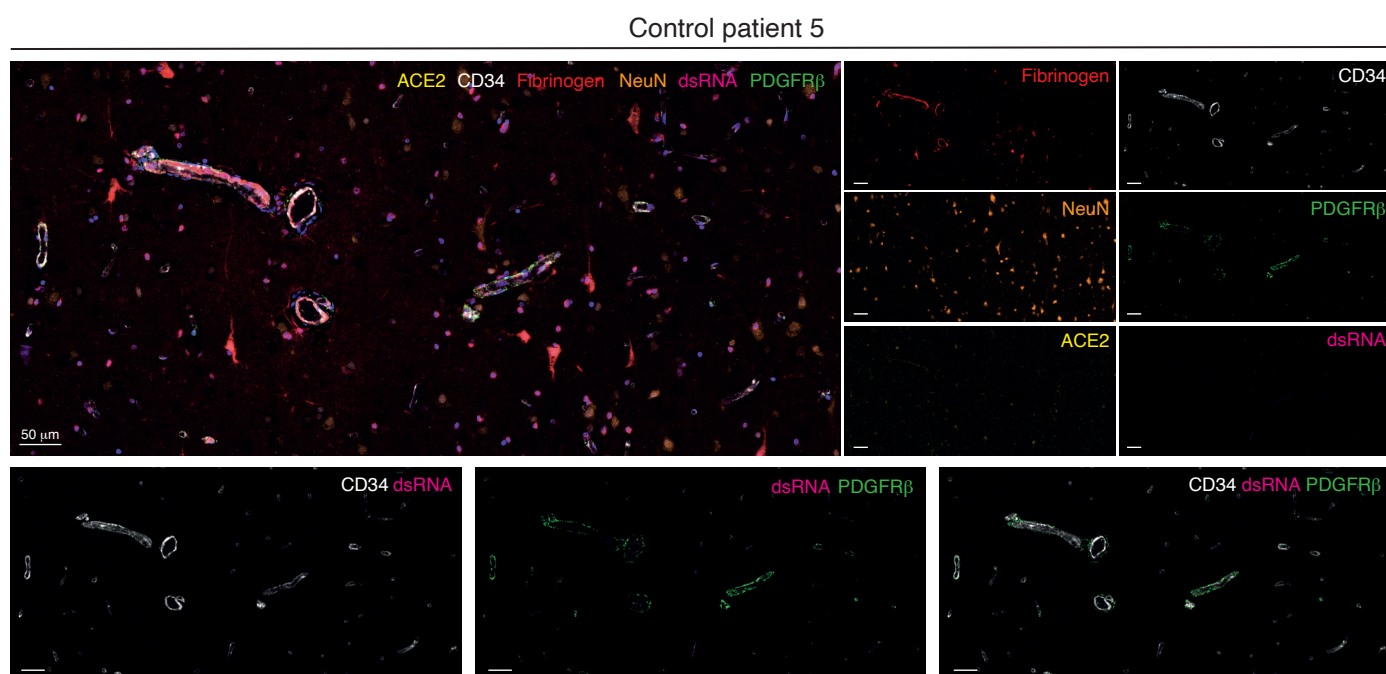
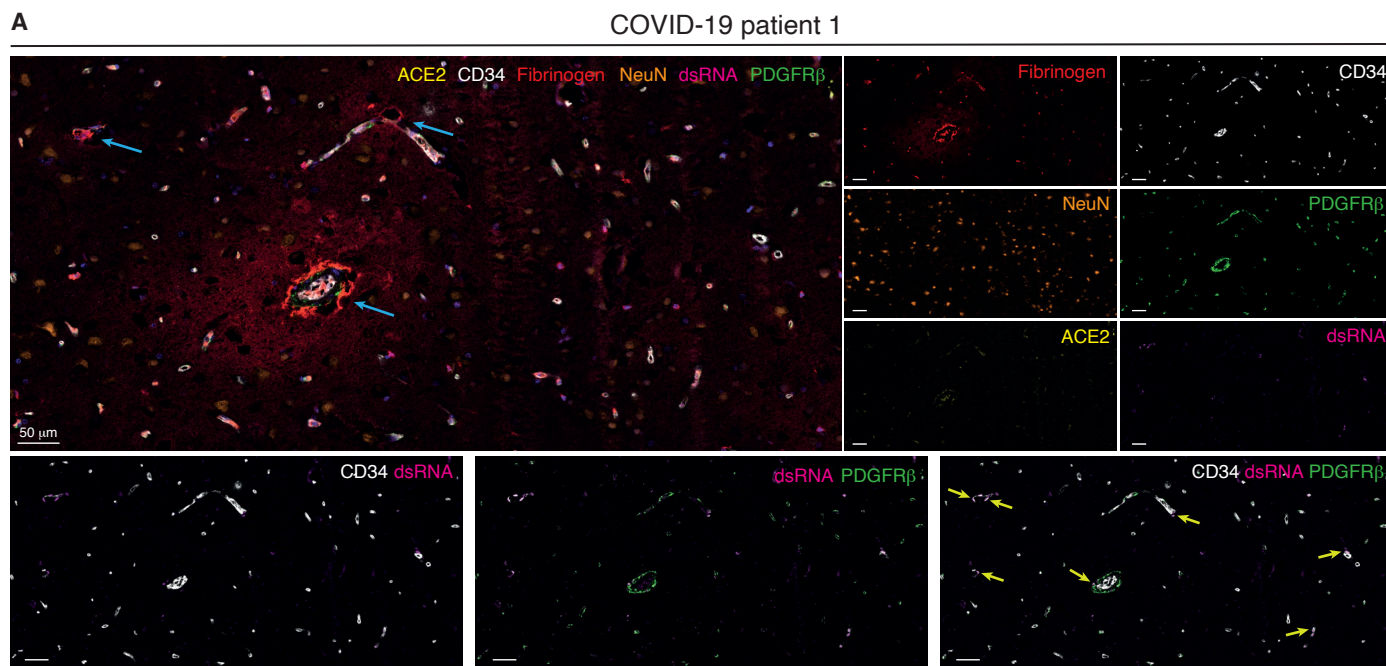
Supplementary Figure 2 (A) Additional field of the 7-plex mIHC staining panel of placental tissue infected with SARS-CoV-2 presented in Figure 2D. The magenta arrows indicate accumulation of viral dsRNA in correspondence of the ACE2-positive areas by the specialized epithelial layer of syncytiotrophoblast in the placenta. The intensity of each OPAL fluorophore is further presented in individual photomicrographs. **(B)** Immunohistochemical detection of viral components and dsRNA in a COVID-19-infected placenta and in a normal placental specimen. Cell nuclei are counterstained with hematoxylin (blue). **(D)** Multiplex IHC fields of the peri-vascular immune cell infiltration in the frontal cortex of two COVID-19 patients. The antibody panel was designed for the concomitant detection of CD34 (endothelium) and five immune cell markers: CD4 (T helper cells), CD8 (cytotoxic T lymphocytes), CD20 (B cells), CD68 (macrophages), and FOXP3 (regulatory T cells). Individual OPAL intensities are displayed as “pathology view”, in which the fluorescent signal is transformed into a digitalized chromogenic DAB-like deposit.

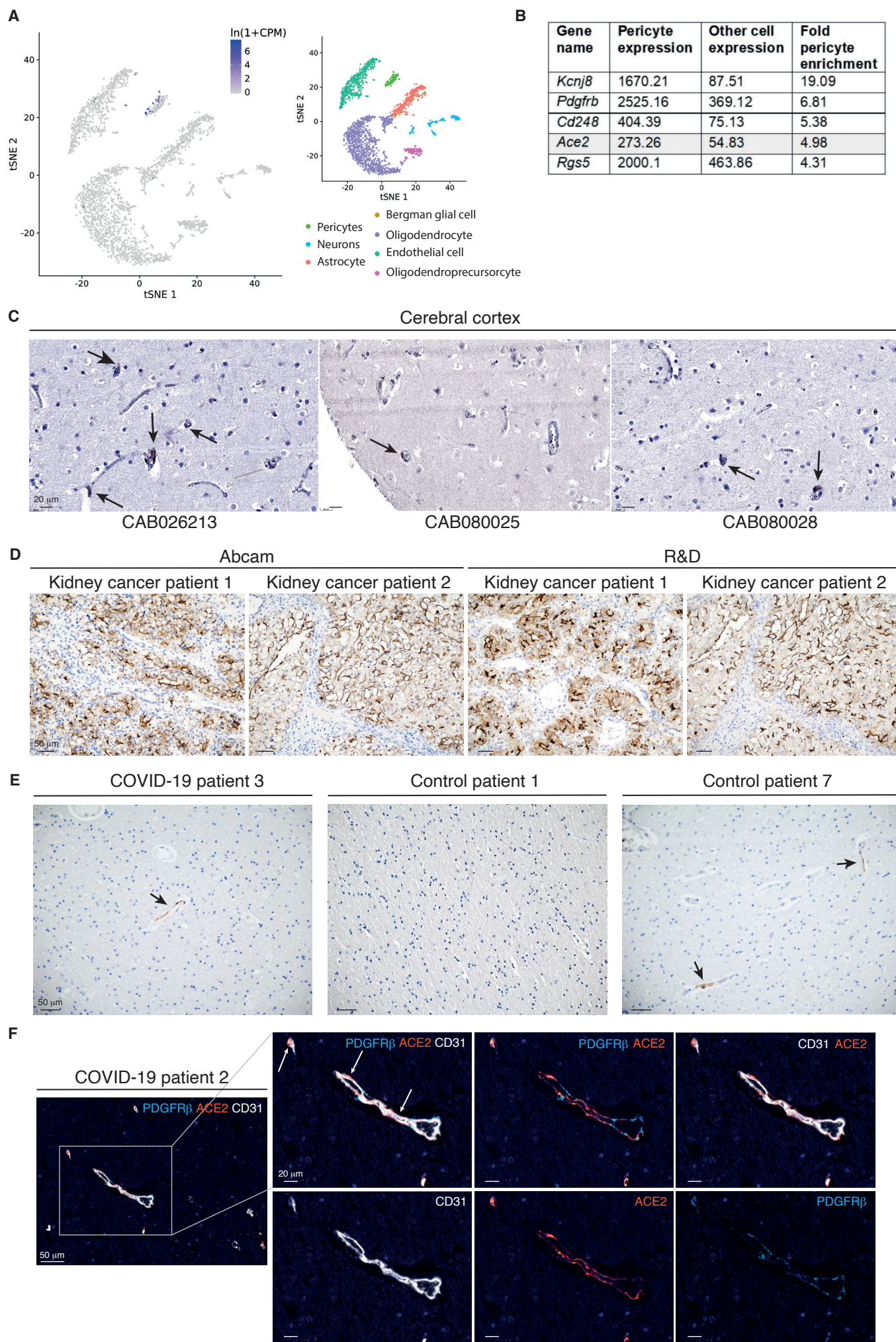
Supplementary Figure 3 (A) Representative IHC of fibrinogen staining in the brain of a COVID-19 patients and in control tissue. Cell nuclei are counterstained with hematoxylin

(blue). **(B)** Additional field of the composite mIHC in the COVID-19 patient presented in Figure 3A. The fields depict the neurovascular unit (CD34, PDGFR β , and ACE2), fibrinogen, viral dsRNA, and neurons. The cyan arrows indicate fibrinogen leakage. The intensity of each OPAL fluorophore is further presented in individual photomicrographs. **(C)** Individual OPAL intensities of the two panels presented in Figure 3A are displayed as “pathology view”, in which the fluorescent signal is transformed into a digitalized chromogenic DAB-like deposit.



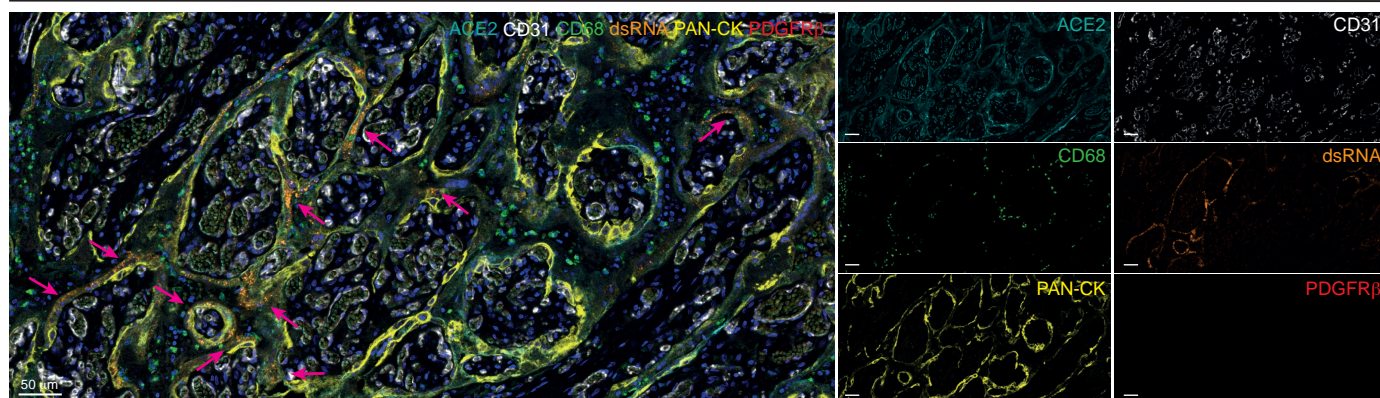




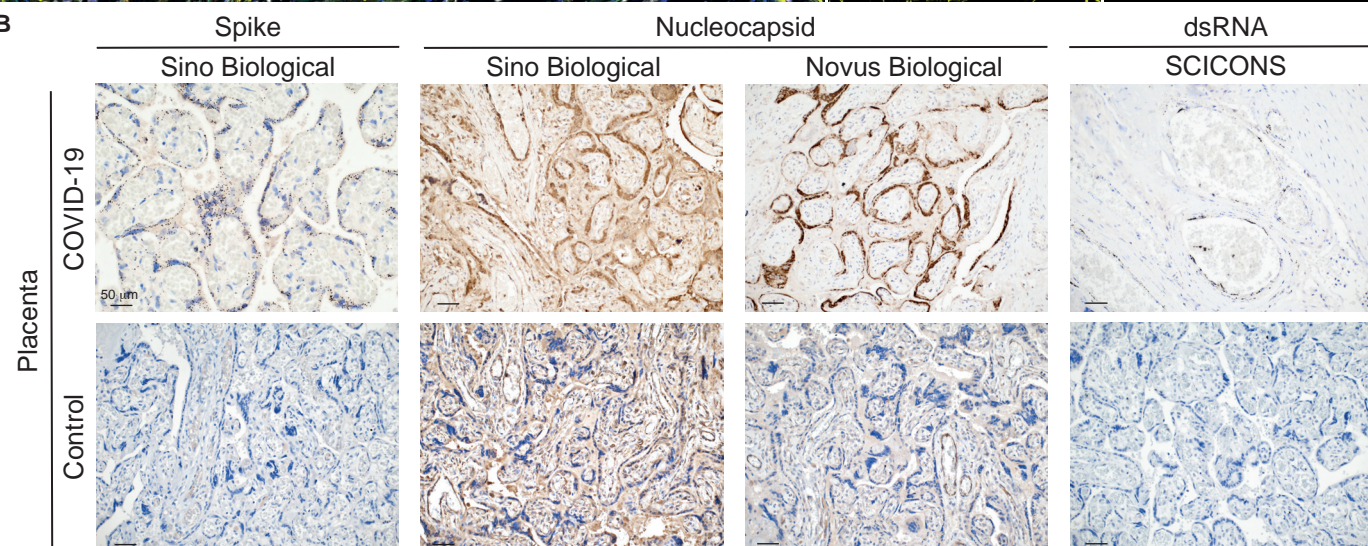


A

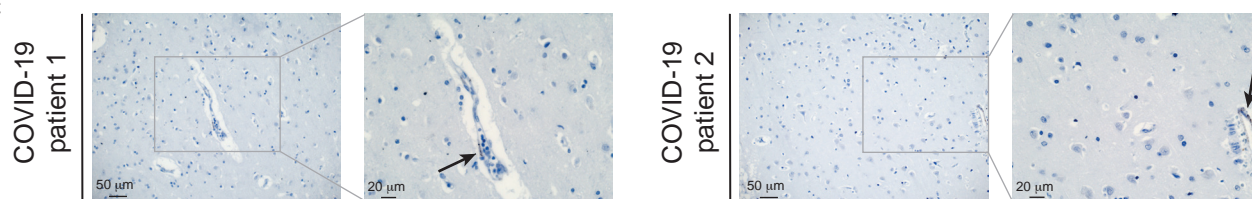
Placenta COVID-19



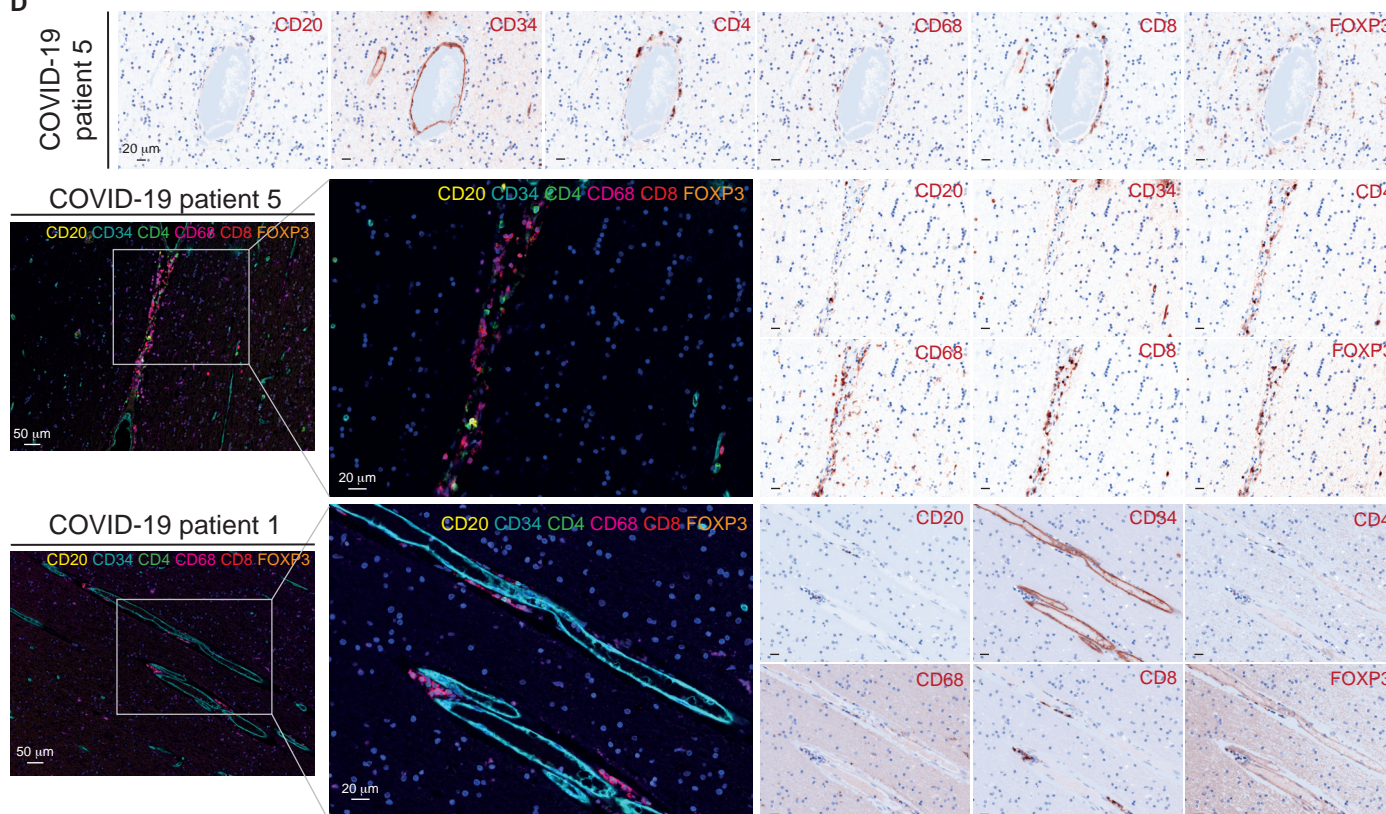
B

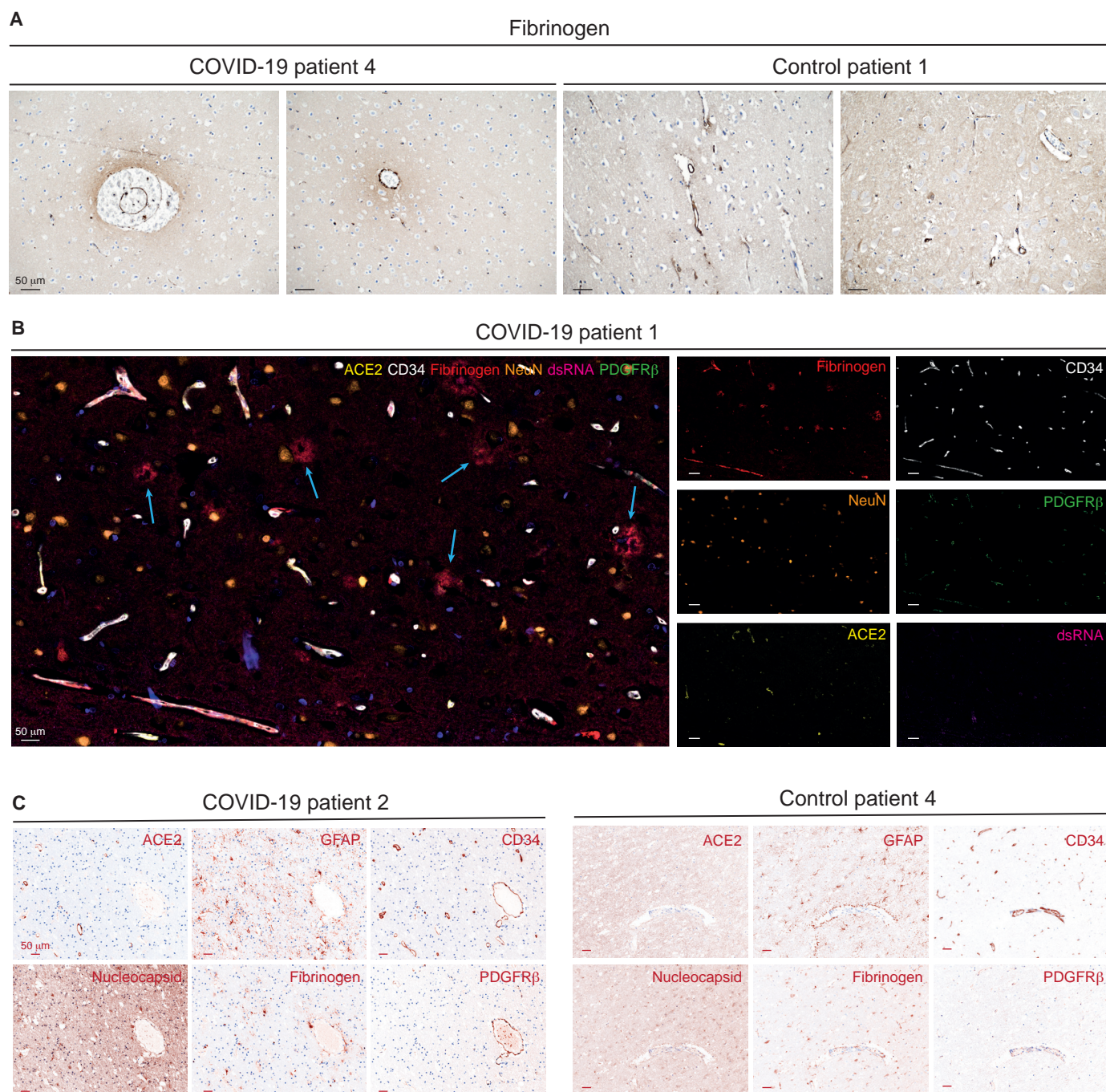


C



D





Supplementary Table 1 Characteristics of the COVID-19 patients and relative controls (brain and placenta IHC/mIHC study, Lund University)

Patient ID	Age (years)	Gender	ACE2	Vascular histopathological evaluation	Neurological assessment
COVID-19 1	67	M	High	Small vessel disease, signs of cerebral hypoperfusion	Unconscious >4 weeks before death
COVID-19 2	54	M	High	Mild but general edema of CNS	Unconscious >4 weeks before death
COVID-19 3	72	M	Moderate	No remarks	Unconscious >1 week before death
COVID-19 4	80	M	Not detected	No remarks	Alert except for two days of confusion
COVID-19 5	57	M	Not detected	Perivascular lymphocytic infiltration/vascular thrombosis	Alert until death
COVID-19 6	75	F	Not detected	No remarks	Alert until death
Control 1	73	M	Not detected	No remarks	No remarks, Alert until death
Control 2	68	F	High	Hypertensive angiopathy and microthrombosis	Decline before death
Control 3	72	F	Low	Severe vascular/ischemic lesions	No remarks
Control 4	82	F	High	Progressive multifocal leukoencephalopathy	No remarks
Control 5	37	M	Low	No remarks	Alert until death
Control 6	68	F	Low	Small vessel disease, microbleeds, stroke in brainstem	No remarks
Control 7	29	M	Low	No remarks	No remarks
COVID-19 placenta	27	F	High	Not applicable	Not applicable
Control placenta	28	F	High	Not applicable	Not applicable

Supplementary Table 2 Characteristics of the COVID-19 patients and relative controls (CSF study, Sahlgrenska University hospital, Gothenburg)

Patient ID	Age (years)	Gender	PDGFRβ (pg/ml)	Interval^a (days)	Neurological assessment
COVID-19 CSF 1	84	F	1065	10	Confusion
COVID-19 CSF 2	70	M	459	6	Confusion, fatigue, delayed response to questions
COVID-19 CSF 3	62	M	976	15	Confusion, personality changes, delayed response to questions, disorientation
COVID-19 CSF 4	64	M	275	7	Altered consciousness/somnolence, neck stiffness, photophobia
COVID-19 CSF 5	42	M	602	12	Exhaustion, dysgeusia
COVID-19 CSF 6	72	M	772	12	Confusion, delayed response to questions
COVID-19 CSF 7	59	F	678	13	Confusion, fatigue, dysarthria, myoclonus
COVID-19 CSF 8	78	F	611	10	Confusion
Control CSF 1	72	F	1308	Not applicable	Not applicable
Control CSF 2	76	M	1938	Not applicable	Not applicable
Control CSF 3	56	M	705	Not applicable	Not applicable
Control CSF 4	72	M	738	Not applicable	Not applicable
Control CSF 5	47	M	1246	Not applicable	Not applicable
Control CSF 6	73	M	1051	Not applicable	Not applicable
Control CSF 7	59	F	905	Not applicable	Not applicable
Control CSF 8	67	F	941	Not applicable	Not applicable

^aDays between the initial report of COVID-19 symptoms and the lumbar puncture.

Supplementary Table 3 Antibody list

Target	Manufacturer	Article number	Host	Reactivity	Clonality	Dilution	HIER ^a	Application
ACE2	Abcam	Ab108252	Rabbit	Human, Mouse, Rat	Monoclonal EPR4435[2]	1:100	Citrate buffer (pH6)	IHC/mlIHC
ACE2	R&D	MAB933	Mouse	Human, Hamster	Monoclonal 171606	1:50	Tris-EDTA buffer (pH9)	IHC
CD4	Akoya Biosciences	Kit: OP7TL4001KT		Human		70 ng/ml	Tris-EDTA buffer (pH9)	mlIHC
CD8	Akoya Biosciences	Kit: OP7TL4001KT		Human		120 ng/ml	Tris-EDTA buffer (pH9)	mlIHC
CD20	Akoya Biosciences	Kit: OP7TL4001KT		Human		100 ng/ml	Citrate buffer (pH6)	mlIHC
CD31	Cell Signaling Technology	3528S	Mouse	Human	Monoclonal 89C2	1:1000	Citrate buffer (pH6)	mlIHC
CD34	Novus Biologicals	NBP2-32932	Mouse	Human, Primate	Monoclonal QBEnd/10	1:1000	Citrate buffer (pH6)	mlIHC
CD68	Akoya Biosciences	Kit: OP7TL4001KT		Human		15 ng/ml	Citrate buffer (pH6)	mlIHC
dsRNA	SCICONS	10010200	Mouse	Virus	Monoclonal J2	1:500	Tris-EDTA buffer (pH9)	IHC/mlIHC
Fibrinogen	Abcam	Ab189490	Rabbit	Human, Mouse, Rat	Monoclonal EPR18145-84	1:4000	Tris-EDTA buffer (pH9)	IHC/mlIHC
FOXP3	Akoya Biosciences	Kit: OP7TL4001KT		Human		700 ng/ml	Citrate buffer (pH6)	mlIHC
GFAP	Atlas Antibodies	HPA056030	Rabbit	Human, Mouse		1:2500	Citrate buffer (pH6)	IHC/mlIHC
NeuN/RBFOX3	Atlas Antibodies	HPA030790	Rabbit	Human	Polyclonal	1:200	Citrate buffer (pH6)	mlIHC
pan-CK	Akoya Biosciences	Kit: OP7TL4001KT		Human		400 ng/ml	Citrate buffer (pH6)	mlIHC
PDGFR β	Cell Signaling Technology	3169S	Rabbit	Human, Mouse, Rat	Monoclonal 28E1	1:75	Tris-EDTA buffer (pH9)	mlIHC
SARS-CoV nucleocapsid	Novus Biologicals	NB100-56576SS	Rabbit	Virus	Polyclonal	1:100	Citrate buffer (pH6)	IHC/mlIHC
SARS-CoV-2 nucleocapsid	Sino Biologicals	40143-019	Rabbit	Virus	Monoclonal 019	1:100	Citrate buffer (pH6)	IHC
SARS-CoV-2 spike	GeneTex	GTX135356	Rabbit	Virus	Polyclonal	1:100	Citrate buffer (pH6)	IHC/mlIHC
SARS-CoV-2 spike	Sino Biological	40150-R007	Rabbit	Virus	Monoclonal 007	1:100	Citrate buffer (pH6)	IHC/mlIHC

^aHIER: heat-induced epitope retrieval

Supplementary Table 4 Multiplex IHC panels

Panel	Position 1	Position 2	Position 3	Position 4	Position 5	Position 6
Neurovascular unit (Fig. 1E)						
HIER ^a /Stripping	pH9	pH6	pH6			
Blocking		10 min, RT				
Primary antibody	PDGFR β	ACE2	CD31			
Dilution	1:75	1:100	1:1000			
Incubation (time, temperature)		30 min, RT				
OPAL	OPAL 480	OPAL 620	OPAL 690			
Dilution	1:100	1:100	1:100			
Incubation (time, temperature)		10 min, RT				
Panel	Position 1	Position 2	Position 3	Position 4	Position 5	Position 6
Placenta (Fig. 2B)						
HIER/Stripping	pH9	pH9	pH6	pH6	pH6	pH6
Blocking			10 min, RT			
Primary antibody	dsRNA	PDGFR β	ACE2	Pan-CK	CD68	CD31
Dilution	1:500	1:75	1:100			1:1000
Incubation (time, temperature)			30 min, RT			
OPAL	OPAL 480	OPAL 520	OPAL 570	OPAL 620	OPAL 690	OPAL 780
Dilution	1:100	1:50	1:50	1:50	1:50	1:25
Incubation (time, temperature)			10 min, RT			
Panel	Position 1	Position 2	Position 3	Position 4	Position 5	Position 6
Immunology (Fig. 2E)						
HIER/Stripping	pH9	pH9	pH6	pH6	pH6	pH6
Blocking			10 min, RT			
Primary antibody	CD4	CD8	CD20	FOXP3	CD68	CD34
Dilution	70 ng/ml	120 ng/ml	100 ng/ml	700 mg/ml	15 ng/ml	1:1000
Incubation (time, temperature)			30 min, RT			
OPAL	OPAL 520	OPAL 570	OPAL 540	OPAL 620	OPAL 650	OPAL 690
Dilution	1:50	1:50	1:50	1:50	1:50	1:50
Incubation (time, temperature)			10 min, RT			
Panel	Position 1	Position 2	Position 3	Position 4	Position 5	Position 6
Fibrinogen (Fig. 3A)						
HIER/Stripping	pH9	pH9	pH9	pH6	pH6	pH6
Blocking			10 min, RT			
Primary antibody	dsRNA	PDGFR β	Fibrinogen	ACE2	NeuN	CD34
Dilution	1:500	1:75	1:4000	1:100	1:200	1:1000
Incubation (time, temperature)			30 min, RT			
OPAL	OPAL 480	OPAL 520	OPAL 570	OPAL 620	OPAL 690	OPAL 780
Dilution	1:100	1:50	1:50	1:50	1:50	1:25
Incubation (time, temperature)			10 min, RT			
Panel	Position 1	Position 2	Position 3	Position 4	Position 5	Position 6
Astrocytes (Fig. 3B)						
HIER/Stripping	pH9	pH9	pH6	pH6	pH6	pH6
Blocking			10 min, RT			
Primary antibody	PDGFR β	Fibrinogen	ACE2	GFAP	CoV-2 spike	CD34
Dilution	1:75	1:4000	1:100	1:2500	1:100	1:1000
Incubation (time, temperature)			30 min, RT			
OPAL	OPAL 520	OPAL 570	OPAL 540	OPAL 620	OPAL 650	OPAL 690
Dilution	1:50	1:50	1:50	1:50	1:50	1:50
Incubation (time, temperature)			10 min, RT			

^aHIER: heat-induced epitope retrieval